ELSEVIER

NeuroImage

www.elsevier.com/locate/ynimg
NeuroImage 22 (2004) 42–56

Analysis of neural mechanisms underlying verbal fluency in cytoarchitectonically defined stereotaxic space—The roles of Brodmann areas 44 and 45

Katrin Amunts,[a,*] Peter H. Weiss,[a,b] Hartmut Mohlberg,[a] Peter Pieperhoff,[a,c] Simon Eickhoff,[a] Jennifer M. Gurd,[d,e] John C. Marshall,[d] Nadim J. Shah,[a] Gereon R. Fink,[a,b] and Karl Zilles[a,f]

[a] *Institut für Medizin, Forschungszentrum Jülich GmbH, Jülich, Germany*
[b] *Neurologische Klinik, RWTH Aachen, Germany*
[c] *Klinik für Psychiatrie und Psychotherapie der Universität Düsseldorf, Düsseldorf, Germany*
[d] *Neuropsychology Unit, University Department of Clinical Neurology, Radcliffe Infirmary, Oxford, UK*
[e] *Psychology Department, University of Hertfordshire, Hertfordshire, UK*
[f] *C. & O. Vogt Institut für Hirnforschung, Universität Düsseldorf, Düsseldorf, Germany*

Received 15 April 2003; revised 14 November 2003; accepted 30 December 2003

We investigated neural activations underlying a verbal fluency task and cytoarchitectonic probabilistic maps of Broca's speech region (Brodmann's areas 44 and 45). To do so, we reanalyzed data from a previous functional magnetic resonance imaging (fMRI) [Brain 125 (2002) 1024] and from a cytoarchitectonic study [J. Comp. Neurol. 412 (1999) 319] and developed a method to combine both data sets. In the fMRI experiment, verbal fluency was investigated in 11 healthy volunteers, who covertly produced words from predefined categories. A factorial design was used with factors verbal class (semantic vs. overlearned fluency) and switching between categories (no vs. yes). fMRI data analysis employed SPM99 (Statistical Parametric Mapping). Cytoarchitectonic maps of areas 44 and 45 were derived from histologic sections of 10 postmortem brains. Both the in vivo fMRI and postmortem MR data were warped to a common reference brain using a new elastic warping tool. Cytoarchitectonic probability maps with stereotaxic information about intersubject variability were calculated for both areas and superimposed on the functional data, which showed the involvement of left hemisphere areas with verbal fluency relative to the baseline. Semantic relative to overlearned fluency showed greater involvement of left area 45 than of 44. Thus, although both areas participate in verbal fluency, they do so differentially. Left area 45 is more involved in semantic aspects of language processing, while area 44 is probably involved in high-level aspects of programming speech production per se. The combination of functional data analysis with a new elastic warping tool and cytoarchitectonic maps opens new perspectives for analyzing the cortical networks involved in language.

Keywords: Brodmann's areas; fMRI; Cytoarchitectonic study; Verbal fluency

Introduction

Broca first conjectured that the posterior part of the left inferior frontal gyrus was crucially implicated in the production of "articulate language" (Broca, 1861). This conclusion was based on both clinical and neuropathologic, macroscopic examination of an aphasic patient who became known as "Tan Tan" (Signoret et al., 1984). The behavioral syndrome described has subsequently been called "Broca's aphasia". Tan Tans's lesion involved the posterior part of the inferior frontal gyrus where the opercular and triangular parts are found (Duvernoy, 1991). Broca did not analyze Tan Tan's brain or those of his subsequent patients with respect to microstructure and also refrained from relating lesions to cortical areas. Considering the location of the lesions in these historical brains (Castaigne, 1979; Signoret et al., 1984), it has been hypothesized that Brodmann (1909) areas (BA) 44 and 45 are the cytoarchitectonic correlates of Broca's region (Aboitiz and Garcia, 1997; Uylings et al., 1999).

Recent functional imaging techniques allow the neural substrate of language to be investigated in healthy subjects (for an overview, see Bookheimer, 2002). For example, verbal fluency, in the sense of producing a series of words from a predefined category, a task which is often impaired in Broca's aphasia (e.g., Goodglass et al., 1967) and which may involve functional distinctions such as different grammatical classes (Caramazza, 2000), has frequently been analyzed with both positron emission tomography (PET) and functional magnetic resonance imaging (fMRI) (Audenaert et al., 2000; Ravnkilde et al., 2002; Schlosser et al., 2002). More specific aspects of language perception and production such as phonologic and syntactic processing (Ben-Shachar et al., 2003; Clahsen and Featherstone, 1999; Featherstone et al., 2000; Friederici et al., 2003; Groß et al., 1998; Indefrey et al., 2001; Keller et al., 2001; Knösche et al., 2000; Mecklinger et al., 1995) have also been explored using functional imaging. Such studies increased our knowledge of neurolinguistic aspects of language processing. They do not, however, answer the

* Corresponding author. Institut für Medizin, Forschungszentrum Juelich GmbH, D-52425 Juelich, Germany. Fax: +49-2461-61-8307.
E-mail address: k.amunts@fz-juelich.de (K. Amunts).
Available online on ScienceDirect (www.sciencedirect.com.)

1053-8119/$ - see front matter © 2004 Elsevier Inc. All rights reserved.
doi:10.1016/j.neuroimage.2003.12.031

question which cortical areas participate in the various aspects of language processing.

There is, at present, no way to analyze function and microstructure in one and the same human brain, although some very recent, high-resolution MR studies with a spatial resolution at almost microscopic level are promising in that respect (Barbier et al., 2002; Fatterpekar et al., 2002; Walters et al., 2003). At present, the anatomical interpretation of functional activations is typically based on the atlas system of Talairach and Tournoux (1988), which uses Brodmann's schematic surface drawings of an architectonic map (Brodmann, 1909) as the basis for an architectonic parcellation. Thus, Brodmann's areas were simply transferred to the atlas brain by trying to identify corresponding sulcal patterns in both brains, assuming a strong association between the sulcal pattern and the borders of the cortical areas. Such an association, however, was already doubted by Brodmann himself. He mentioned that "...a schematic drawing can reflect only the major spatial relationships, and therefore, precise topographic associations cannot be considered in general or only in a distorted manner; this is true in particular for all those cortical regions which have borders in the neighborhood of sulci and those regions which are located in the depths of such a cortical region" (translated from Brodmann, 1908).

We have previously been able to confirm that this statement is true for the vast majority of cytoarchitectonic areas, for example, of the parietal lobe, motor, visual and temporal cortex (for overviews, see Amunts et al., 2002; Zilles et al., 2002a,b), and for BA 44 and 45 in particular (Amunts et al., 1999). Although both areas always occupy the posterior part of the inferior frontal gyrus, the precise locations of their borders vary considerably. For example, BA 44 occupies in most of the cases the opercular part, but can also encroach on the triangular part. BA 45 is located at the triangular part, but may also reach aspects of the opercular part. BA 44 may border BA 6 in the anterior or in the posterior bank of the fundus of the precentral sulcus (Amunts et al., 1999). BA 45 may occupy parts of the middle frontal gyrus (Rajkowska and Goldman-Rakic, 1995). In addition to the variability of areal borders with respect to sulci, there also exists a large intersubject variability of the sulcal pattern of the frontal lobe itself (Ono et al., 1990; Tomaiuolo et al., 1999).

To overcome these problems, cytoarchitectonic probability maps of BA 44 and 45 (Amunts et al., 1999) have been developed for structural–functional analysis of language (Horwitz et al., 2003; Indefrey et al., 2001). Such analysis, however, is dependent on the precision of the localization of functional activations with respect to the cytoarchitectonic parcellation of the cerebral cortex. At least two methodologic aspects are crucial in this context: (i) the application of a common reference brain for both the fMRI in vivo and the postmortem cytoarchitectonic data, and (ii) a uniform warping approach to the common reference brain of all data modalities irrespective of the different quality and spatial resolution [in vivo, functional echo planar imaging (EPI), and structural anatomical, as well as postmortem, cytoarchitectonic data].

The aim of this combined anatomical and fMRI study was to test the hypothesis that cytoarchitectonically-defined BA 44 and 45 of the left hemisphere are involved differentially in a verbal fluency task in healthy volunteers. To test this hypothesis, we combined and reanalyzed data from a previous fMRI study of verbal fluency (Gurd et al., 2002) and of the cytoarchitecture of BA 44 and 45 (Amunts et al., 1999). To answer the neuroscientific question, we approached the methodologic problems outlined above by developing and applying a method for the integration of fMRI data analyzed using SPM99 (Statistical Parametric Mapping) with a non-SPM, elastic warping algorithm, and probabilistic cytoarchitectonic maps. The present study, thus, not only combines fMRI data with probabilistic cytoarchitectonic maps, but also presents a new methodologic approach to analyzing the relationship of cortical microstructure and cerebral function.

Material and methods

Cytoarchitectonic mapping of BA 44 and 45

Mapping was performed in cell-body stained (Merker, 1983), serial histologic sections of 10 human brains (5 males, 5 females; age range from 37 to 85 years; mean age = 66 years, SD = 14 years). All brains were obtained from body donor programs in accordance with the ethics committee of the University of Düsseldorf. The autopsies were performed within 8 to 24 h after death. Handedness and language dominance of the subjects were not known. Considering an incidence of about 95% of left-sided language dominance (Branche et al., 1964), it is likely that most of our cases were dominant for the left side. Brains were fixed in 4% formalin (cases nos. 2–8) or in Bodian, a mixture of formalin, glacial acetic acid, and ethanol (remaining cases). MR imaging of the fixed brains was carried out with a Siemens 1.5 T magnet (Erlangen, Germany), with a T_1-weighted three-dimensional (3-D) FLASH sequence covering the entire brain (flip angle, 40°; repetition time of TR = 40 ms; echo time of TE = 5 ms for each image). Each volume consists 128 sagittal sections. The spatial resolution was 1 × 1 × 1.17 mm, each voxel with a resolution of 8 bits corresponding to 256 gray values.

The brains were embedded in paraffin and sectioned in the coronal plane through both hemispheres. Per brain, 6000–7500 sections (20 μm) were acquired. Each 15th section was mounted on glass slides and silver-stained for perikarya (Merker, 1983). Each 60th section of the entire series was used for further analysis of cytoarchitecture. Images of these histologic sections were digitized and three-dimensionally reconstructed.

Accordingly, each brain was represented by three data sets: (i) the histologic data set with high contrast, but distortions caused by histologic techniques (images of histologic, silver-stained sections were digitized with a CCD camera), (ii) a photo-data set with low contrast (resulting from the unstained surface of the paraffin block) showing the histologic section before sectioning, together with a reference system to establish the 3-D integrity of the histologic volume, and (iii) the structural MR-data set which was obtained before paraffin-embedding with improved contrast but at a different orientation than the photo-data set (Schormann et al., 1995). The comparison of these three data sets allowed us to correct for deformations and shrinkage inevitably caused by histologic techniques, for example, embedding, sectioning, and mounting on glass slides. Both linear and nonlinear transformations were applied (Henn et al., 1997; Mohlberg et al., 2003; Schormann and Zilles, 1998).

To account for intersubject variability in brain macroscopy, brains were warped to the standard format of the ECHBD (European Computerized Human Brain Data Base) reference brain (Roland and Zilles, 1994, 1998) using a combination of an affine transformation (only shifting, scaling, and rotating), a normalization of grey levels, and subsequent nonlinear, elastic transformation (Henn et al., 1997; Mohlberg et al., 2002; Schormann and Zilles, 1998). A vector field φ was calculated for each

data set which described the transformation of each voxel of the transformed brain (value and direction) to the reference brain (for more details of the transformation, see below). The final orientation of the brains was in the plane determined by the anterior–posterior commissures, that is, the AC–PC plane. The final resolution of both the reference brain and the postmortem brains was 1 × 1 × 1 mm.

Cytoarchitectonic borders of BA 44 and 45 (Fig. 1) were defined using an observer-independent approach for the definition of areal borders (Amunts et al., 1999; Schleicher et al., 1999; Zilles et al., 2002b). This approach is based on (i) the measurement of the grey level index (GLI; Schleicher and Zilles, 1990) as an estimate of the volume fraction of nerve cell bodies (Wree et al., 1982), (ii) the calculation of profiles which quantify the laminar changes in the volume fraction from the cortical surface to the white matter, that is, the cytoarchitecture, and which cover in small equidistant intervals the putative border regions of the cytoarchitectonic areas, (iii) the extraction of features from the profiles as numerical descriptors of the cytoarchitecture, (iv) the calculation of the Mahalanobis distances as measures of differences in shape between profiles coming from different areas, (v) the definition of areal borders at those locations at which the Mahalanobis distances show significant values, thus indicating that the shape of the profile, that is, the cytoarchitecture, has changed abruptly.

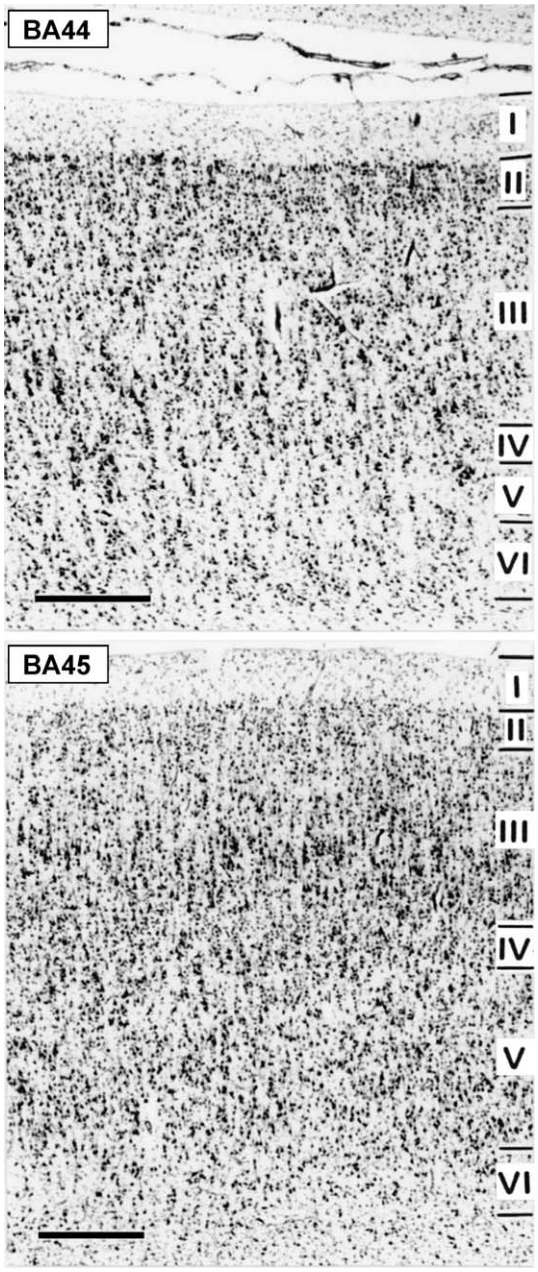

Fig. 1. Cytoarchitecture of BA 44 and 45 in coronal, cell-body stained sections of a postmortem brain. The cytoarchitecture of both areas is characterized by large pyramidal cells in deep layer III, which exceed those of layer V in size. Whereas granular BA 45 shows a clearly visible layer IV, the layer IV of the dysgranular BA 44 is thinner and not clearly delineable from neighboring layers, since pyramidal cells from layers III and V invade into layer IV. Cortical layers are numbered. Scale bars, 0.5 mm.

Areal borders were then transferred to digitized histologic sections and three-dimensionally reconstructed (Fig. 2). The reconstructions of the two areas in the postmortem brains showed that both areas occupied the posterior part of the inferior frontal gyrus in each brain (Fig. 2). They also revealed a considerable intersubject variability, which can be characterized in three different ways: (i) the shape and the extent of both areas on the free cortical surface was variable. Compare, for example, the appearance of BA 44 in the right hemisphere of brain no. 7 with that of the right BA 44 of brain no. 1 and the left BA 44 of brain no. 3; (ii) the relationship of the cytoarchitectonically defined borders with respect to surrounding sulci was clearly variable. For example, whereas the diagonal sulcus marked the border between BA 44 and 45 in the right hemisphere of brain no. 3, this sulcus was inside of BA 44 in left brain no. 8, and it was completely absent in brain no.10; and (iii) brain macroscopy (i.e., the shape and presence of the sulci) was also variable. For example, the diagonal sulcus was present in only every second hemisphere.

The individual cytoarchitectonic maps of BA 44 and 45 were then warped to the standard reference brain using the vector field φ as calculated for the transformation of the individual postmortem brains. Centers of gravity of the maps and the extent in all spatial directions were calculated for each area of each postmortem brain and averaged over the whole sample size (Tables 1 and 2). Finally, the cytoarchitectonic maps were superimposed upon the reference brain. Color-coded ‘‘probability maps’’ were calculated which showed, for each voxel of the reference brain, the number of brains in which the cytoarchitectonically defined areas overlapped (Fig. 3). Such a probability map represents a measure of intersubject variability in the size and location of the respective cytoarchitectonic area under the assumptions that the intersubject variability in the sulcal and gyral pattern of the brain has been eliminated after applying the elastic warping procedure, and that the influence of the warping itself can be neglected.

Functional imaging of verbal fluency

fMRI of verbal fluency (Gurd et al., 2002) was performed in 11 right-handed healthy volunteers (6 male, 5 female; mean age: 32 years, SD = 4 years) with no history of neurologic or psychiatric disease. The investigation was approved by the ethics committee of the Heinrich Heine University of Düsseldorf. Informed consent was obtained before MR imaging. In contrast to the previous study (Gurd et al., 2002), (i) we here focus on verbal fluency (and not

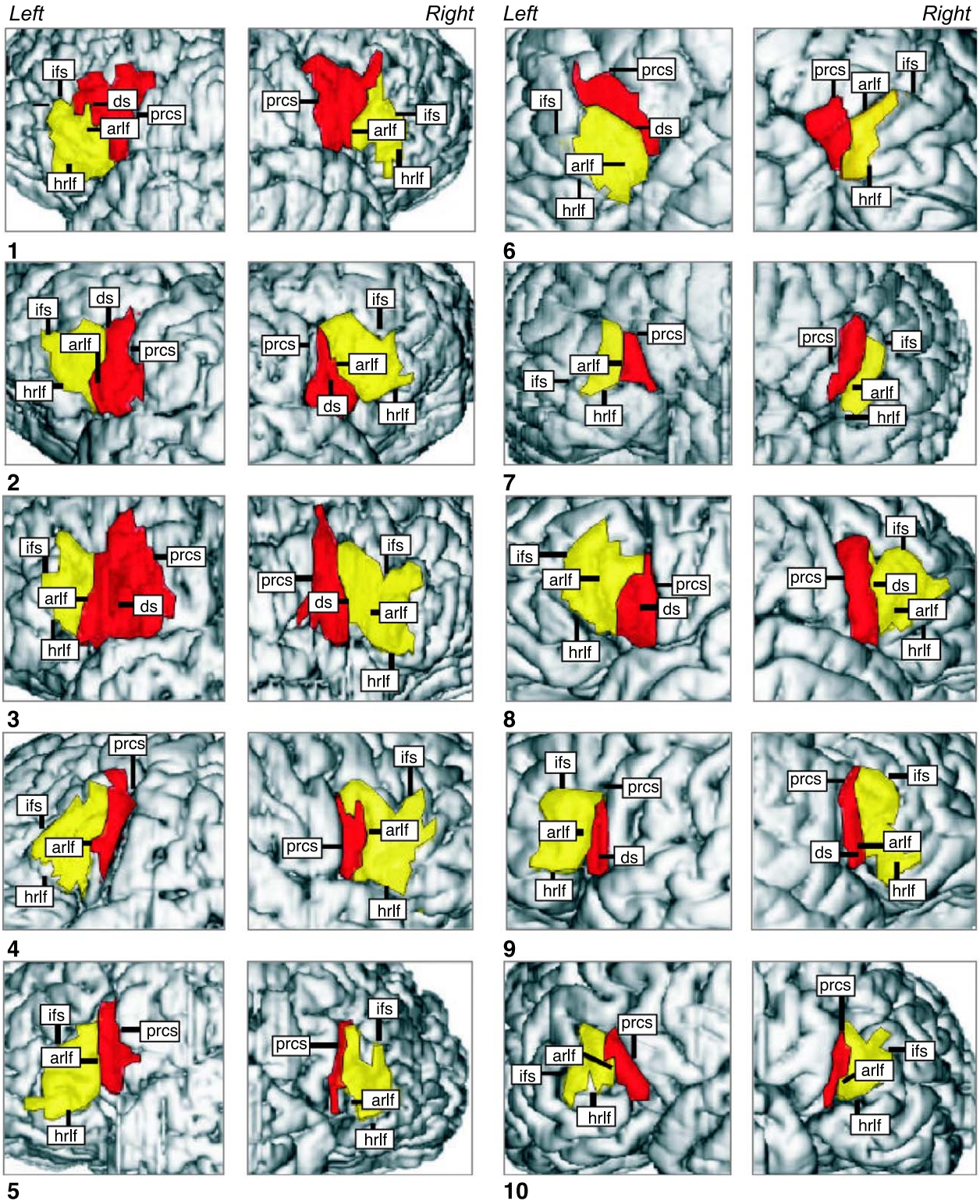

Fig. 2. Lateral views of 3D reconstructions (surface rendering) of 10 individual postmortem brains (nos. 1–10) with BA 44 (red) and 45 (yellow) of the left and right hemispheres after cutting into histological sections, staining for cell bodies, and observer-independent definition of cytoarchitectonic borders on serial histological sections (Amunts et al., 1999). arlf, denotes ascending branch of the lateral fissure; ds, diagonal sulcus; hrlf, horizontal branch of the lateral fissure; ifs, inferior frontal sulcus; prcs, precentral sulcus. Note the high intersubject variability with respect to (i) differences in shape and size of both areas, (ii) variability in the sulcal pattern, and (iii) in the relationship of areal borders to surrounding sulci.

Table 1
Means centers of gravity of BA 44 and 45 in standard stereotaxic space with standard deviations (in parentheses; $n = 10$)

	BA 44		BA 45	
	Left	Right	Left	Right
x	−42 (2)	49 (2)	−42 (2)	48 (1)
y	11 (7)	14 (6)	24 (7)	27 (4)
z	20 (4)	21 (4)	17 (5)	18 (4)

x is the distance in millimeters to the right (+) or left (−) of the midsagittal (interhemispheric) line; y is the distance anterior (+) or posterior (−) to the vertical plane through the anterior commissure; and z is the distance above (+) or below (−) the intercommissural line.

switching), and (ii) we reanalyze the data to allow for a topographic interpretation of the functional activations on the basis of probabilistic maps of BA 44 and 45 (rather than anatomical landmarks, i.e., gyri and sulci). We, therefore, provide a quantitative measure for the involvement of these two cortical areas in verbal fluency. This reanalysis, extension and new approach, involves the application of a different normalization procedure (warping) and a different reference brain for the MR data. Furthermore, we use a different statistical approach for analyzing the functional activations based on the focus on BA 44 and 45 [“ROI (region of interest) analysis”], which are the areas of interest with respect to the neuroscientific question under investigation.

The design of the fMRI study was, in short, as follows: subjects were asked to covertly produce words with their eyes closed. In the nonswitching trials of this verbal fluency task, subjects responded with a series of items from a prespecified semantic category (“semantic”; e.g., flowers or furniture) or from overlearned sequences (“overlearned”; e.g., months of the year or days of the week). The contrast between these two verbal fluency tasks enabled us to image brain regions implicated in the task with the greater semantic search requirements. In the switching conditions, subjects produced words alternately from three semantic categories (e.g., fruits, cars, or furniture) or from three overlearned sequences (e.g., days of the week, months, or letters of the alphabet). The comparison of these switching trials with the single, no-switching trials should isolate those regions implicated in switching between verbal categories. The latter condition is not of primary relevance for the purpose of the current study. The design of the experiment was thus factorial—factor 1 was verbal category (semantic vs. overlearned); factor 2 was switching, that is, single specification fluency was compared with alternating specification fluency (switching vs. nonswitching).

All subjects were pretrained on all these types of verbal fluency tasks to ensure that the experimental results reflect task performance per se, rather than the effects of learning novel tasks. Training was performed both several days before scanning and a day before scanning. For more details of the training, see Gurd et al. (2002). Immediately before scanning, subjects received a final training session with overt task performance recorded on tape to assess task performance.

MRI was performed on a Magnetom Vision 1.5 Tesla scanner. Anatomical T_1-weighted images covering the whole brain were obtained using a high-resolution MP-RAGE pulse sequence [repetition time (TR) = 11.4 ms; echo time (TE) = 4.4 ms; flip angle = 15°; field of view = 230 mm; matrix size = 200 × 256; 128 sagittal slices with 1.25-mm slice thickness]. EPI was performed with a gradient booster system. Pulse sequence parameters were as follows: gradient echo EPI, TE = 66 ms; TR = 5 s; 32 slices with 4.0-mm slice thickness; interslice gap = 0.3 mm. The blocked design fMRI paradigm comprised eight repetitions of a 45-s baseline state and a 30-s activation state (two repeats of each of the four experimental conditions). The baseline consisted 30 s (6 images) without presentation of auditory task instructions and 15 s (3 images) with presentation of auditory task instructions. During the activation state, six whole-brain images were acquired. Each volunteer performed all five runs, whereby each run comprised the eight blocks mentioned above during the complete measurement procedure.

Image processing

Statistical analysis and image processing were performed on SPARC Ultra 10 workstations (SUN Microsystems Computers, Palo Alto, USA) using MATLAB (The Mathworks Inc., Natick, USA), the MPItool (MPItool, MPI for Neurological Research, Cologne, Germany), and Statistical Parametric Mapping software (SPM99, Wellcome Department of Cognitive Neurology, UK; http://www.fil.ion.ucl.ac.uk). The MPItool was applied for data transformation into SPM (analyze format). SPM99 was used for coregistration of the EPI images to their anatomical images, smoothing, and creation of statistical maps of significant relative regional BOLD (blood oxygenation level dependent) response changes (Friston et al., 1995a,b). The 120 volume images of each time series were automatically realigned to the first image to correct for head movement between scans. Image sets of the four conditions and the baseline were then coregistered to the 3-D anatomical data set using SPM.

We applied a non-SPM elastic warping algorithm to enable the transformation of (i) the postmortem data, (ii) the anatomical MR data, and (iii) the EPI data of the verbal fluency task to a non-SPM reference (ECHBD) brain (Roland and Zilles, 1994, 1998). Data were thereafter expressed in terms of standard stereotaxic coordinates in the x-, y-, and z-axes. The application of a non-SPM warping algorithm required the export of the anatomical 3-D and EPI data from SPM, and the transformation of these data into the space of ECHBD reference brain. The non-SPM warping algorithm was used to allow for the preservation of the details of the anatomy of the brains as a necessary condition for warping anatomical data sets to an individual reference brain.

The anatomical 3-D brain data of each subject were interactively separated from surrounding tissue (e.g., meninges and cerebrospinal fluid). This careful segmentation was an important prerequisite for a precise warping to the reference brain (Henn et

Table 2
Means extents of BA 44 and 45 in standard stereotaxic space with standard deviations (in parentheses; $n = 10$) and corresponding data of the brain of Talairach and Tournoux (1988)

		BA 44		BA 45	
		Left	Right	Left	Right
x	Mean extent	28 (5)	23 (4)	21 (3)	21 (5)
	Talairach atlas	5	–	5	–
y	Mean extent	21 (6)	18 (5)	27 (5)	25 (6)
	Talairach atlas	9	–	20	–
z	Mean extent	36 (7)	35 (7)	33 (6)	35 (5)
	Talairach atlas	25	–	20	–

Coordinates as above.

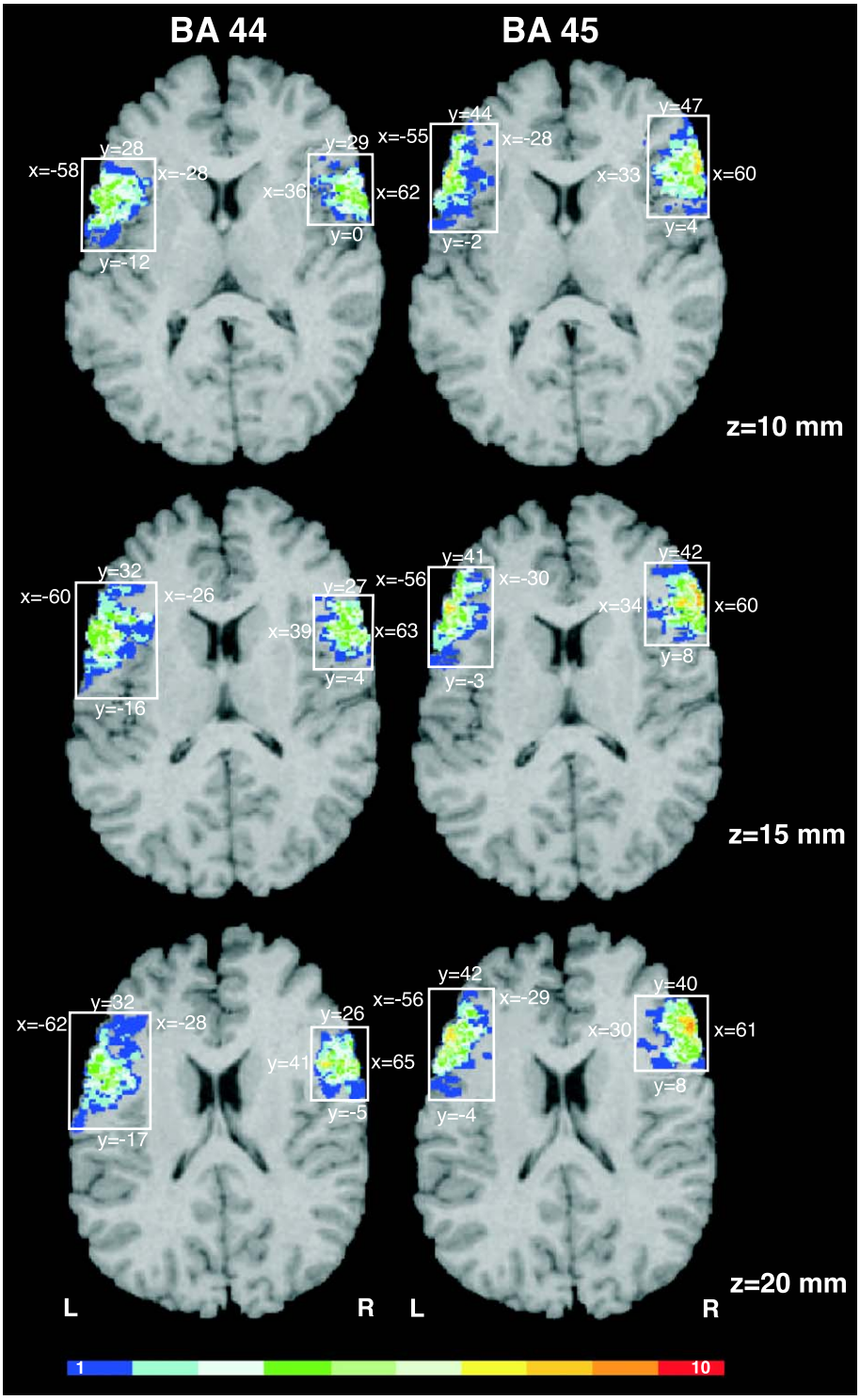

Fig. 3. Probability maps of BA 44 (left column) and 45 (right column) at three exemplary horizontal sections: z = 10, 15, and 20 mm of standard reference space (Roland and Zilles, 1994). The number of overlapping brains in each voxel of the standard brain is color-coded; for example, yellow means an overlap of 7 of 10 brains; dark orange, an overlap of 9 of 10 brains. The maximal extent in x and y direction of all 10 brains with respect to the line crossing the interhemispheric fissure at the level of the anterior commissure is given in mm (Talairach and Tournoux, 1988). Note the considerable intersubject variability in the location and extent of both areas as reflected by the high proportion of blue and green pixels which represent low overlap, that is, high variability. Left in the image is left in the brain.

al., 1997; Mohlberg et al., 2002; Schormann and Zilles, 1998). Warping was done by using a volumetric deformation process D which is based on maximizing locally the image similarity between a template T and a reference data set R (i.e., the individual ECHBD reference brain): D: $T \rightarrow R$. Voxels from the template were deformed to the voxels of the reference with a 3-D elastically

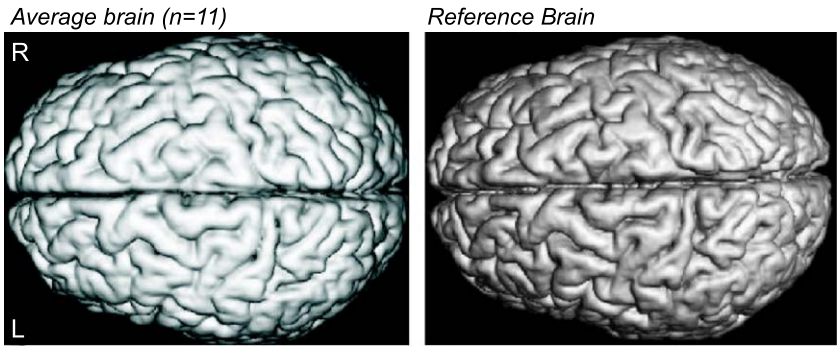

Fig. 4. Surface renderings of an average of 11 in vivo brains after nonlinear registration (left) to the reference brain (right). View from dorsal. The crispness of the average brain, reconstructed from all individuals after nonlinear registration, reflects an exquisite registration accuracy.

deformable model. These deformations were generated from translation groups applied for each voxel of T:

$$D: \vec{x} = (x_1, x_2, x_3) \rightarrow (x_1 - u_1(\vec{x}), x_2 - u_2(\vec{x}), x_3 - u_3(\vec{x}))$$

The deformation field $\vec{u}(\vec{x})$ was calculated by minimizing the image intensity difference for each point $\vec{x}$ of the volume:

$$D(\vec{x}) = \frac{1}{2}\int_{\text{Volume}} (R(\vec{x}) - T(\vec{x} - \vec{u}(\vec{x})))^2 \mathrm{d}\vec{x}$$

yielding a local intensity force:

$$\vec{f}(\vec{u}(\vec{x})) = (T(x - \vec{u}(\vec{x})) - R(\vec{x})) \cdot \nabla T(\vec{x} - \vec{u}(\vec{x})).$$

Using a physical model based on an energy function which is deduced from the well-known continuum mechanics theory of Navier-Lamé, smoothness constraints between T and R are simultaneously satisfied:

$$\mu \cdot \Delta \vec{u}(\vec{x}) + (\lambda + \mu)\nabla(\nabla \cdot \vec{u}(\vec{x})) = \alpha \cdot f(\vec{u}(\vec{x})).$$

The physical properties of the elastic model and therefore the quality of the deformation process can be appropriately controlled through the constants γ, μ, and α. The latter partial differential equation consisting approximately 36 million (number of voxels multiplied by the number of dimensions) unknowns cannot be calculated analytically. Therefore, we used a numerical approach that determined the solution by an iterative algorithm. To reduce the computational burden, an optimized full-multigrid method was implemented. Three different scales were used in this study, corresponding to the original image resolution (high), a subsampled version by a factor 2 (middle), and a subsampled version by a factor 4 (low). The transformation vector field using an ordinary iterative numerical algorithm for solving large equation systems was calculated for each resolution. The results obtained in low resolution were up-sampled and linearly interpolated to the next higher spatial resolution. The up-sampled transformation vector field was then used as the initialization for the studied resolution. The calculation of a precise warp of a single subject brain of 256 × 256 × 256 voxels on a Linux PC with a 1 GHz Intel Pentium CPU, resulting in a deformation field φ that transforms each voxel of the anatomical scan to its corresponding reference brain voxel, takes about 3.5 h, whereby an extremely high accuracy in superposition of different individuals was achieved (Fig. 4).

The EPI images were spatially normalized to the standard reference brain by using the corresponding vector field φ, reduced

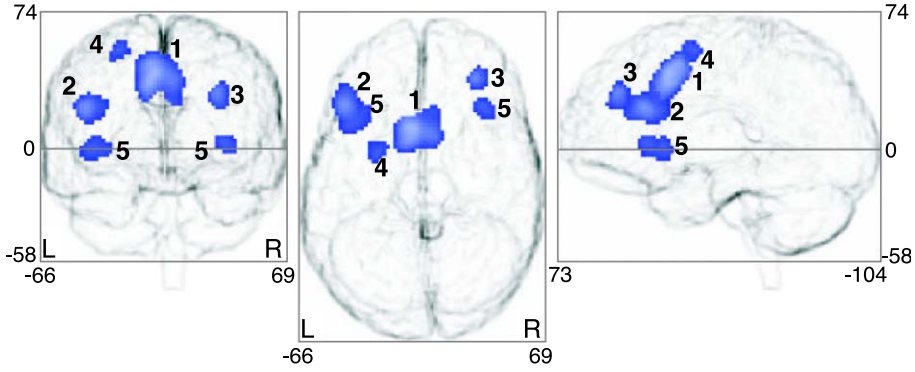

Fig. 5. Relative differential increase in neural activity for the 11 subjects associated with semantic relative to overlearned fluency. Areas of significant increase in neural activity are shown as through-projections onto representations of the standard reference brain (Roland and Zilles, 1994). For the calculation of these increases, anatomical MR data sets and EPI data were both warped to this standard reference brain using a novel nonlinear, elastic warping algorithm (Mohlberg et al., 2002) which is based on a movement model for large deformations and a full multigrid procedure (Henn et al., 1997; Schormann and Zilles, 1998). The exact coordinates of the local maxima (identified by numbers) within the areas of activation and their Z statistics are given in Table 4. The topographical relationship of the local maxima with respect to cytoarchitectonic areas BA 44 and 45 is shown in Fig. 6. L, R denote left and right hemispheres, respectively.

Table 3
Relative differential increases in brain activity during covert word retrieval against baseline for 11 subjects in the format of the standard reference brain (Roland and Zilles, 1994)

Region	Hemisphere	x	y	z	Z score
Precentral gyrus/ prefrontal cortex	L[a]	−54	−6	40	7.52
	R	48	−2	34	5.90
Insula/orbitofrontal cortex	L	−34	14	2	5.95
	R	32	26	2	6.19
Cerebellum	L	−30	−56	−30	5.95
	R	30	−56	28	5.88
Middle frontal gyrus	R	34	36	24	5.70
Posterior parietal cortex	R	−26	−72	42	5.58

Whole brain analysis. Stereotaxic coordinates and designation as in Table 1.
[a] Overlap of the cluster with cytoarchitectonically defined BA 44 and 45 (see Fig. 6).

to 2 × 2 × 2 mm voxel size, and reimported into SPM for smoothing and statistical analysis.

Statistical analysis of fMRI data

Statistical analysis was performed using a random effects model, modeling the different conditions as reference waveforms. Repeated measures (scans) were collapsed within subject to give one scan per condition per subject. These conditions were then compared between subjects, thereby effecting a random effects model. Specific effects were tested by applying appropriate linear contrasts to the parameter estimates for each condition, resulting in a t statistic for each voxel (Friston et al., 1995b). These t statistics constitute a statistical parametric map which was then interpreted by referring to the probabilistic behavior of Gaussian random fields as described by Worsley et al. (1996). For an orientating whole-brain analysis, voxels were identified as significant if they passed a height threshold of $T = 5.09$ ($P < 0.05$, corrected for whole-brain volume) and belonged to a cluster of at least 20 activated voxels. All significant activations are reported in Table 3 for data comparison. Z values are provided to enable comparison with other studies.

As the aim of this study was to examine the involvement of BA 44 and 45 in verbal fluency, the further analysis was restricted to anatomically defined ROIs. These ROIs were defined (separately for the left and right hemispheres) by the combined extent of the unthresholded cytoarchitectonically derived probability maps of BA 44 and 45. For a given number of resels (i.e., resolution elements), a height threshold for the SPM{T} map can be determined, which equals a P level of less than 0.05, corrected for multiple comparisons in the search volume. For the left hemispheric ROI, this height threshold was 3.77. For the right hemispheric ROI, $T = 3.72$. No extent threshold was applied for the ROI analyses.

Data were analyzed with respect to the main effects of verbal class (semantic vs. overlearned fluency) and switching (yes vs. no). A masking procedure was employed to ensure not only that the activations of experimental interest were positive with respect to the other experimental conditions, but also that they were positive with respect of the low-level baseline. Accordingly, (semantic > overlearned) and (overlearned > semantic) were masked with (semantic > baseline) and (overlearned > baseline), respectively.

Finally, the locations of the regions activated were compared with the probabilistic cytoarchitectonic maps of BA 44 and 45 (Fig. 6). For visualization, the probability maps of BA 44 and 45 were thresholded at 50%; that is, only those voxels are shown, which belong to the respective area in 5 or more out of the 10 brains. These volumes represent the "core" of the respective areas.

Results

Cytoarchitectonic mapping of BA 44 and 45

Table 1 shows the stereotaxic coordinates of BA 44 and 45 as obtained by the observer-independent analysis of cytoarchitectonic borders in coronal, cell-body stained sections of 10 human postmortem brains (Amunts et al., 1999). The coordinates show a larger mediolateral, ventrodorsal, and rostrocaudal extent of both left areas than those reported in the atlas of Talairach and Tournoux (1988) (Table 2). Differences between the two maps range from 7 mm (rostrocaudal extent of left BA 45) to 23 mm (mediolateral extent of left BA 44). The individual location and extent of both areas in the postmortem brains were highly variable as demonstrated by the probability maps (Fig. 3).

Neural activations

The whole-brain analysis of the comparison of verbal fluency against low-level baseline (all conditions vs. rest) resulted in bilateral activations of the posterior part of the frontal cortex, including the frontal gyrus, precentral gyrus, parietal lobe, the orbitofrontal gyrus/insula, as well as the cerebellum with more extensive activations on the left than on the right (Table 3).

The ROI analysis showed activations of the left inferior frontal gyrus which included both BA 44 and 45 (Fig. 6); 65% of BA 44

Table 4
Relative differential increases in brain activity during covert word retrieval from semantic category and overlearned sequence fluency for 11 subjects in the format of the standard reference brain (Roland and Zilles, 1994)

Region	Hemisphere	x	y	z	Z score
Semantic > overlearned fluency					
Anterior cingulate cortex[1]	L	−4	12	40	6.43
	R	4	20	24	5.02
Ventral bank of the inferior frontal sulcus[2,a]	L	−42	26	22	5.91
Middle frontal gyrus[3]	R	30	40	30	5.70
Superior frontal gyrus[4]	L	−24	−2	54	5.13
Orbitofrontal cortex[5]	R	34	24	2	5.12
	L	−38	14	0	5.05
(Semantic, nonswitching > overlearned, nonswitching) > (semantic, switching > overlearned, switching)					
Frontal cortex, orbital gyri[6]	L	−20	32	−10	5.18

Whole brain analysis. Stereotactic coordinates as in Table 1. Identification of anatomical regions in accordance to this reference brain. R and L indicate left and right hemispheres, respectively. The superscript numbers refer to the labeling of areas of activation as illustrated in Fig. 5 (for superscript numbers 1 to 5) and Fig. 7 (for superscript number 6).
[a] Overlap of the cluster with cytoarchitectonically defined BA 45, but not BA 44.

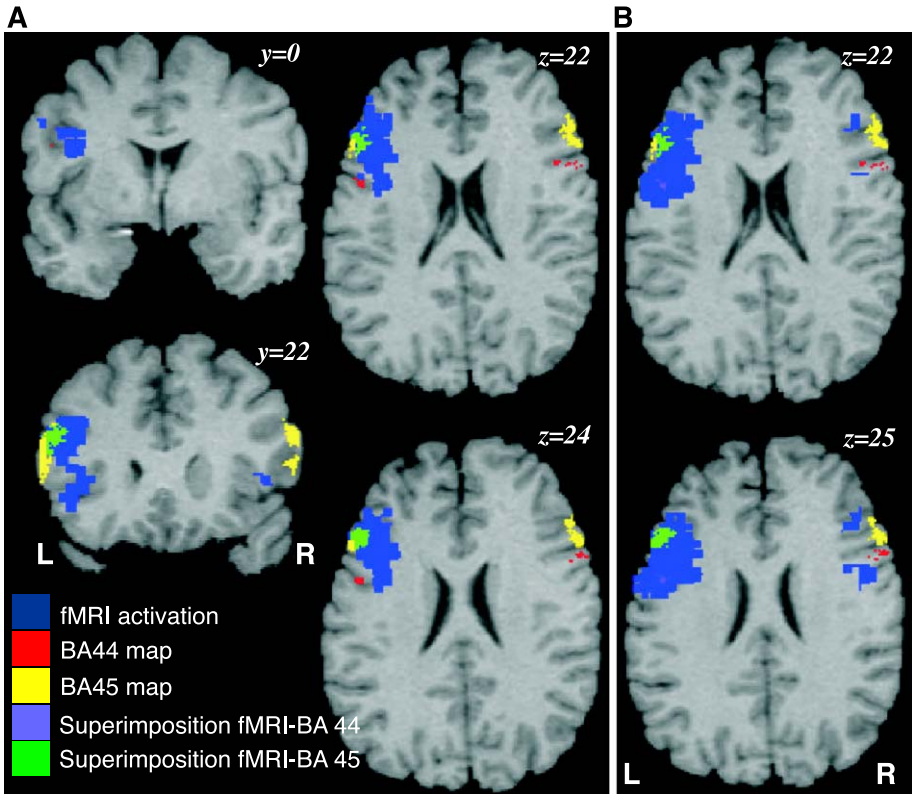

Fig. 6. Superimposition (violet and green) of cytoarchitectonically defined BA 44 (red) and 45 (yellow) with relative differential increases in neural activity for 11 subjects (blue) as shown on representations of the standard reference brain in stereotactic space (Roland and Zilles, 1994). A, semantic versus overlearned fluency; B, all conditions versus rest. The clusters of significant relative increase ($P < 0.05$, corrected for multiple comparisons using small-volume correction) in neural activity were superimposed on horizontal and coronal sections of the standard reference brain. The results for both ROI analyses (left and right hemisphere) are projected simultaneously. R indicates right; L, left hemisphere. The cytoarchitectonic maps of BA 44 and 45 were obtained by (i) superimposing the individual cytoarchitectonic maps in the format of the reference brain, and (ii) selecting only those voxels, which were present in 5 or more out of 10 brains of each area. See Table 2 for coordinates of centers of gravity of the cytoarchitectonic representations.

and 56% of BA 45 were activated (both maps thresholded at 5/10 brains). The corresponding local maximum showed a probability of 60% of lying in BA 45 and of only 20% of lying in BA 44; it was located at $x = -42$, $y = 26$, $z = 22$ ($T = 7.6$). A large cluster of activation was found in the right hemispheric ROI. One of the local maxima of this activation was located at $x = 40$, $y = 24$, $z = 6$ ($T = 6.5$). It showed a probability of 20% of lying in BA 45. The other local maxima showed a lower probability of lying in either BA 45 or 44. In addition, smaller clusters of activations showed a probability of no more than 10% of lying in either BA 44 or 45.

Table 4 shows the regions that were differentially activated as a main effect of semantic category fluency (semantic, nonswitching + semantic, switching > overlearned, nonswitching + overlearned, switching), as assessed in the whole-brain analysis.

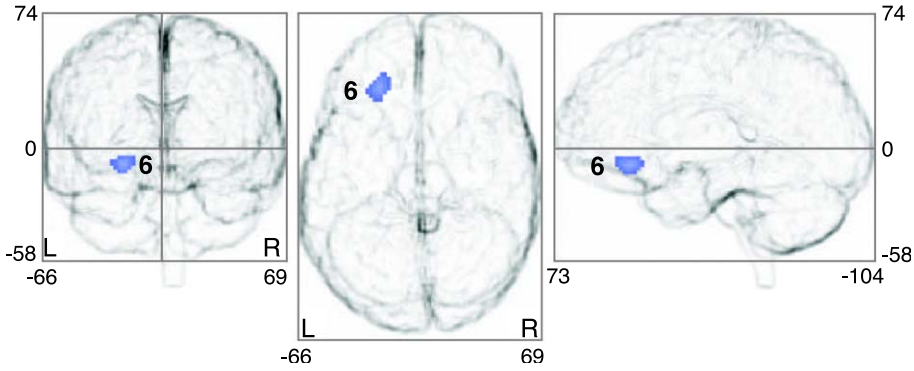

Fig. 7. Relative differential increase in neural activity as interaction (semantic, nonswitching > overlearned, nonswitching) > (semantic, switching > overlearned, switching), showing the involvement of the orbitofrontal cortex of the left hemisphere. Area of significant increase in neural activity is shown as through-projections onto representations of the standard reference brain (Roland and Zilles, 1994). Designation as in Fig. 5. For coordinates of local maxima (numbered by 6) and their Z statistics, see Table 4.

Bilateral activations were observed in the anterior cingulate cortex, the orbital part of the inferior frontal gyrus, in the left superior frontal, right middle frontal, and the left frontal gyrus. The main effect of semantic fluency versus overlearned fluency is shown in Fig. 5.

In the ROI analysis of the left hemisphere, four clusters of activation reached significance. Three of them were negligibly small (<6 voxels). The main cluster of activation (1297 voxels) overlapped mainly with left BA 45 (Fig. 6): 53% of BA 45 and 14% of BA 44 were activated (both maps were thresholded at 5/10 brains). A local maximum within this cluster ($x = -42$, $y = 26$, $z = 22$; $T = 7.5$) was located in BA 45 with a probability of 60%, while its probability of lying in BA 44 was only 20%. Two additional, single-voxel activations ($x = -46$, $y = 6$, $z = 22$; $T = 4.0$, and $x = -44$, $y = 6$, $z = 34$; $T = 3.9$) had a probability of 50% for being located in BA 44. A further cluster of six voxels (maximum at $x = -52$, $y = 0$, $z = 36$; $T = 3.9$) showed a probability of 20% for lying in BA 44. In the right hemispheric ROI, two activations were found (local maxima at $x = 38$, $y = 20$, $z = 6$; $T = 5.0$, and $x = 36$, $y = 32$, $z = 28$; $T = 4.6$). Both local maxima were well outside the centers of BA 44 and 45. The maximal probability for them was only 10% for BA 44 and 0% for BA 45.

The reverse comparison (overlearned, nonswitching + overlearned, switching > semantic, nonswitching + semantic, switching) did not reveal any significant activation.

The second main effect, switching (semantic, switching + overlearned, switching > semantic, nonswitching + overlearned, nonswitching), showed bilateral activation of the superior parietal lobule. No other region was activated in this comparison (Gurd et al., 2002). In the reverse comparison, that is, nonswitching versus switching, no significant activations were found. Finally, the interaction of semantic/overlearned and switching/nonswitching resulted in an orbitofrontal activation (Fig. 7). This activation did not overlap with either BA 44 and 45; it was located more ventrally.

Discussion

The analysis of verbal fluency

Verbal fluency tasks have often been related to Broca's region. Studies employing PET and fMRI showed the participation of the left inferior frontal gyrus in verbal fluency tests. Since lesions of the (usually left) frontal cortex in patients often result in impaired verbal fluency task performance (Baldo and Shimanura, 1998; Owen et al., 1990), such tests are often used in the clinical environment to measure the integrity and function of the frontal cortex (Audenaert et al., 2000; Curtis et al., 2001; Ravnkilde et al., 2002; Schlosser et al., 2002; Smith et al., 2002; Spence et al., 2000). We accordingly here analyzed the relationship of cortical activations during a verbal fluency task with respect to Broca's region and its putative correlates BA 44 and 45. Considering that, in contrast to severe aphasic impairment on language and speech tasks, preservation of so-called "automatic speech" (such as used in this study) has been reported in patients with aphasia (Albert et al., 1981), we also aimed to analyze the differential relationship of cytoarchitectonically defined BA 44 and 45 with semantic verbal fluency and "automatic" speech.

In this context, it is necessary to discuss verbal fluency in more details. Verbal fluency tasks require the subject to produce as many words as possible from some well-defined category (e.g., animals or words beginning with the letter "s"). In clinical practice, patients are usually required to do so for 30 or 60 s per category. Producing items from relatively large open-ended classes (such as animals) can be contrasted with producing items from small closed classes, such as days of the week or months of the year, whose members and their sequence are usually much overlearned ("automatic" speech).

The more open-ended semantic category tasks (e.g., listing animals) are excellent, relatively pure measures of lexical retrieval. Scoring can be both quantitative (number of words produced per unit time) and qualitative (types of error produced). In healthy elderly people, errors are rare but slowed times are common (Lezak, 1995). Deficits on verbal fluency tasks occur in most aphasic syndromes, including Broca's aphasia, with errors characteristic of the particular aphasia type in question (Goodglass et al., 1967). Importantly, patients with damage to left frontal areas, who are not clinically aphasic, may also show impaired verbal fluency (Janowsky et al., 1989). For the most part, however, errors are perseverative in these cases; that is, the patients repeat previously produced items (Baldo and Shimanura, 1998).

Furthermore, patients with idiopathic Parkinson's disease (who are not demented but have impaired dopaminergic projections to prefrontal cortex) also show deficits in verbal fluency, producing fewer items per unit time. This reduction is not entirely due to peripheral articulatory disorder as the patients' rate of speaking in overlearned fluency tasks (e.g., days of the week) does not correlate significantly with their performance on semantic category fluency tasks (Gurd and Ward, 1989). In that study, both patients and control subjects made a small proportion of repetition errors and out-of-category errors.

In short, then, verbal fluency impairments can be seen not only in patients with Broca's aphasia after left frontal damage, but also in nonaphasic patients with different types of frontal pathology. Verbal fluency tasks primarily assess speed and accuracy of lexical retrieval. It is thus unfortunate that the term "verbal fluency" is also used to refer to rate of spontaneous speech, and articulatory and intonational fluency in utterances. Although impairments of fluency in the latter sense are also characteristic of Broca's aphasia, the verbal fluency tasks with which we are concerned here specifically involve lexical access and retrieval of individual words. Broca (1861) himself believed that the third left frontal convolution (which came to be called Broca's area) was primarily concerned with memory for coordinating speech movements. Later work established that the region was also implicated in lexical retrieval as assessed by the types of verbal fluency tasks we use here (Frith et al., 1991a; Hinke et al., 1993) as well as in syntactic processes (Caplan et al., 2000). Thus, fluency impairments (in the current sense) can be superimposed on the linguistic (including prosodic) deficits of Broca's aphasics (Belin et al., 1996; Goodglass et al., 1967).

The data from verbal fluency tasks used in previous imaging studies show that large parts of the prefrontal cortex, exceeding considerably the classical speech region, are activated. This finding suggests a differential contribution of different cortical areas of the inferior, medial, and superior frontal gyri to semantic and overlearned fluency. In this context, it is also necessary to consider the putative role of working memory, strategic search, error control, and monitoring in these process and their putative respective contribution to the neural activations observed. Clearly, the above-mentioned processes play a role in verbal fluency as studied here. The

question is, however, whether there is a differential involvement of these processes in semantic fluency as compared to overlearned fluency. For example, maintenance in working memory has been shown to be supported by a network of left hemispheric ventral prefrontal, parietal, and motor regions (for an overview, see Fletcher and Henson, 2001). However, we did not observe any differential involvement of, for example, the inferior parietal cortex, which is assumed to play a role in phonologic storage (Paulesu et al., 1993). Further aspects of the relevant discussion have already been provided in our earlier study (Gurd et al., 2002). Likewise, differences in strategic search might be expected when comparing semantic and overlearned fluency. Frith et al. have reported bilateral activations of the dorsolateral prefrontal cortex when generative, random keypressing was compared with reactive, stimulus-driven keypressing (Frith et al., 1991b). Left dorsolateral prefrontal cortex activation was also reported when random number generation was compared with counting (Jahanshahi et al., 2000). Activation of the ventral prefrontal cortex has also been reported with random number generation compared to sequential counting (Jahanshahi et al., 2000). The hypothesis was that prefrontal cortex was involved in maintenance and monitoring processes required during random generation of items. We did not observe activations in these areas in the critical comparisons, but rather in all conditions relative to baseline. With regard to the differential contribution of BA 44 and 45 during semantic verbal fluency, this suggests that working memory load and supervisory processes were not greatly different in semantic fluency versus overlearned fluency. Although we cannot completely rule out the contribution of other factors which are not directly related to semantics' (e.g., differences in strategy, selection), the data are consistent with the hypothesis that greater semantic search is the critical factor in the comparison.

Stereotaxic localization of cytoarchitectonically defined BA 44 and 45

Observer-independent mapping of BA 44 and 45 postmortem brains and subsequent elastic transformation into the stereotaxic space of the reference brain enabled us to calculate probability maps for both areas, containing frequency information about the likely presence of these two areas in each voxel of the reference space. The maps showed a high intersubject variability, both in extent and location. The calculated centers of gravity are within the range of the atlas data of Talairach and Tournoux (1988). Importantly, however, the extent of both areas was considerably larger than the data provided by Talairach and Tournoux (1988) would suggest. This is not surprising, since the Talairach and Tournoux atlas is based on only one left hemisphere (which has not been delineated cytoarchitectonically), whereas the present data rely on cytoarchitectonic delineations of BA 44 and 45 in 20 hemispheres of 10 postmortem brains. The discordance observed was maximal for the mediolateral extent where it reached 23 mm (left BA 44). The extent in the mediolateral direction was more or less arbitrarily estimated by Talairach and Tournoux, since Brodmann's map as their model did not contain any explicit information about the locations of areas within the depths of the sulci and therefore was not helpful for architectonic localization in the mediolateral extent. Finally, stereotaxic coordinates differ between left and right hemispheres. These differences are particularly relevant in language-related areas such as BA 44 and 45.

For one aspect of our structural–functional comparisons, only those parts of the probability maps were considered which coincided topographically in 5 or more of the 10 brains. The criterion for selecting this threshold was to create maps which show similar volumes to the averaged volume of the respective cortical area in a single brain (Amunts et al., 1999). Furthermore, only the selection of a threshold characteristic for a probabilistic map allows one to discuss whether a whole cortical area or some subarea thereof is involved in a particular brain function (e.g., 53% of the voxels of left BA 45 were activated when semantic fluency was compared with overlearned fluency). An alternative approach makes use of the whole probabilistic map (overlap from one to ten brains) and subsequent topographic interpretation of both centers of gravity and maximal activation with respect to this map (e.g., a peak of a cluster was located with a probability of 60% in BA 45). Both approaches were applied in the present study. They reflect different aspects of data analysis—one from the perspective of the cortical area, the other from the perspective of the functional activation—and thus supplement each other. In contrast to the majority of functional imaging studies, where we do not know the "real" extent and volume of a functional activation, and therefore can only refer to statistical (or heuristic) criteria to select thresholds (smoothing sizes, etc.), the volumes of microscopically defined cortical areas can be objectively measured. Thus, the application of cytoarchitectonic maps represents a significant step forward for localizing cortical areas and their involvement in functional observations.

Localization of neural activations as the main effect of semantic category fluency

The increases in neural activity observed overlapped with left BA 44 and 45 when fluency was compared with rest (independently of switching and verbal category). Word production from superordinate categories thus activates both BA 44 and 45. In addition to these areas, other regions of the left and right middle, superior and inferior frontal, and anterior cingulate gyri were activated. When semantic fluency was compared with overlearned sequence fluency and superimposed on the cytoarchitectonic maps, activation of BA 45 was observed, which occupied a large portion of this area. A very small extent of activation was also observed in BA 44. The clusters of activation comprised only a few voxels and hence should be interpreted with caution, since they are below the resolution of the EPI images and smaller than the smoothing filters applied. From a neuroscientific perspective, it is problematic to interpret such small activations, since they suggest that only a relatively small subpopulation of a cortical area participates in a certain brain function. Such an assumption remains to be proven. Therefore, we conclude that there was a crucial differential activation of BA 45.

Activation of Broca's region of the left hemisphere has been reported previously in automatic speech tasks (Bookheimer et al., 2000; Wildgruber et al., 1996) when compared with a low-level baseline. We, therefore, conclude that verbal fluency per se involves both left BA 44 and 45, which is in correspondence with the interpretation of both areas as the anatomical correlates of Broca's region. The areas differ from each other, however, in their participation in semantic processing—left BA 45 is more involved than is BA 44 in verbal fluency tasks with high semantic load.

Evidence concerning a differential involvement of left prefrontal areas in speech production tasks, which draw upon different aspects of semantic and phonologic processing with an anterior/posterior gradient, has been provided in several studies (Buckner et

al., 1995; Crivello et al., 2002; Dapretto and Bookheimer, 1999; Demonet et al., 1996; Fiez, 1997; Mummery et al., 1998; Poldrack et al., 1999; Price, 2000; Thompson-Schill et al., 1997; Vandenberghe et al., 1996; Zatorre et al., 1996). Other language-related functions, for example, syntax processing (Ben-Shachar et al., 2003; Caplan et al., 1999; Dapretto and Bookheimer, 1999; Embick et al., 2000; Indefrey et al., 2001), reading, or repeating single words (Dapretto and Bookheimer, 1999; Fiez, 1997; Mummery et al., 1998), also seem to activate only parts of the inferior frontal gyrus. In contrast to these studies, which related the reported activations either to macroscopic structures such as the opercular and triangular parts of the inferior frontal gyrus, posterior and anterior parts, or which interpret their findings with respect to the Brodmann scheme of the Talairach and Tournoux atlas, we report here "in probabilistic terms" the differential participation of BA 45 in semantic processing.

In addition to BA 45, other frontal regions were activated when semantic category fluency was compared to overlearned fluency. The semantic category fluency task is characterized by increased search processes within the internal lexicon, whereas "automatic" speech minimizes such mechanisms (Gurd et al., 2002). Semantic category fluency may thus be taken as an example of intrinsic generation (Goldman-Rakic, 1987) in which sequences of discrete responses must be made in the absence of any external guidance other than the instructional set and without the possibility of prepreparing particular responses. The generation of such sequences draws heavily upon the prefrontal cortex. Participation of prefrontal cortex was accordingly observed when semantic category fluency was compared with overlearned sequence fluency.

The ventral part of the inferior frontal gyrus was activated bilaterally. These activations may underlie semantic processing common to words and pictures (Vandenberghe et al., 1996) and may also result from aspects of strategic control and on-line retrieval of semantic information (Desmond et al., 1995; Fiez, 1997; Poldrack et al., 1999). The bilateral activations of the anterior cingulate cortex are consistent with the role of this region in response selection and task adherence (Stephan et al., 2003). Semantic category fluency requires more suppression of inappropriate responses and facilitation of a wider range of within-category responses than does overlearned sequence fluency (Paus et al., 1993; Thompson-Schill et al., 1997).

Orbitofrontal activations

The orbitofrontal activation of both hemispheres shown in the interaction term suggests an involvement of this region in semantic processing (Fiez, 1997; Price, 1998; Gurd et al., 2002). Activations of the more ventral parts of the frontal lobe during semantic processing have previously been reported (Audenaert et al., 2000; Blank et al., 2002; Gabrieli et al., 1998; Poldrack et al., 1999). With respect to their intermediate location between BA 45 and 47, activations resulting, for example, from the comparison of semantic and phonologic tasks (double subtraction), have been interpreted as belonging to Brodmann's areas 47 or to 45 (Poldrack et al., 1999). The orbitofrontal activations of the interaction of the present study did not overlap with the cytoarchitectonic maps of BA 44 and 45; they were located more ventrally than the lower borders of both areas. It can, therefore, be argued that the activations belong to more ventrally located areas such as BA 47. Thus, cytoarchitectonic maps have improved the anatomical interpretation of functional clusters of activation in ambiguous locations with respect to two neighboring cortical areas.

Methodologic remarks and conclusions

The following differences were observed between the current study and our previous analysis of the fMRI data (Gurd et al., 2002)—the stereotaxic locations of the centers of gravity differed within the range of a few millimeters; the cerebellar activation reported previously did not survive the threshold in the present study; and the activation of the left middle frontal gyrus reported previously was shifted to a slightly more dorsal position in the superior frontal gyrus. These subtle differences are the result of methodologic changes, which were introduced to increase the preciseness and accuracy of the anatomical interpretation of the functional imaging data. These changes were as follows: (i) the application of cytoarchitectonic probabilistic maps for analyzing structure–functional correlation, (ii) the stereotaxic reference to an alternative standard brain, (iii) the introduction of a non-SPM, elastic warping tool to transform the in vivo MR data into the common reference space, and (iv) an additional ROI-based statistical analysis. Thus, functional (EPI) and anatomical T_1-weighted images of the living human subjects ($n = 11$), as well as anatomical postmortem data sets ($n = 10$) and their cytoarchitectonic areas, were warped into the same reference space, using consistently the same nonlinear warping tool. This strategy minimizes methodical blurs and problems, which may occur, for example, when the analysis of functional data is performed completely in SPM99 (with a SPM reference brain and the implied warping tools), and the processing of the cytoarchitectonic data have been performed with respect to a different reference brain and different warping tools. The aim of our methodologic approach was to reach consistency in the applied methods and standards, rather than to make a methodical comparison with SPM99. The alternative way to reach consistency, that is, the integration of cytoarchitectonic maps into SPM99, appears to be an intriguing future project.

The combination of cytoarchitectonic probabilistic maps with data from functional imaging may improve the topographic interpretation of fMRI data. Higher precision in the topographic analysis of the functional activations is necessary as neurolinguistic and neuropsychologic approaches test more and more specific, detailed aspects of language processing, for example, the neural substrates of particular syntactic rules (Ben-Shachar et al., 2003; Friederici and Mecklinger, 1995; Zurif, 2000). Furthermore, several studies have been performed which suggest the participation of Broca's region in nonlanguage tasks, for example, in motion perception (Binkofski et al., 2000; Koski et al., 2002) and in local search (Manjali et al., 2003). The analysis of whether such different tasks share common neural substrates in Broca's region depends, to a large extent, on the precision with which the topography of the different activations can be defined.

In contrast to the atlas system of Talairach and Tournoux (1988), the present probabilistic maps of cytoarchitectonic areas are based on their microstructural delineation; they contain information about intersubject and interhemispheric differences, show borders between cortical areas, have a higher spatial resolution, and are related to an in vivo reference brain. These advantages make them an appropriate tool for the analysis of structural–functional relationship. Probabilistic maps have not yet been constructed for the whole cerebral cortex. Although some activations observed in the current study could be related precisely to a cortical area; others

(e.g., those of the orbitofrontal gyrus, the middle and superior frontal gyrus) could not. These gaps in the cytoarchitectonic map of the cerebral cortex will be remedied during the next few years. Another problem results from the nature of the maps themselves—they contain frequency-based information about the location of a cortical area. Cortical areas are highly (but to a different degree) variable in size and location. When the applied threshold is too strict, the extent of the cortical areas will be underestimated, and activations, which are located outside the thresholded map, may be interpreted as being outside the area, although in fact, they still belong to it. Vice versa, if one analyzes the relationship of an activation with respect to the whole probabilistic map, one may get several topographic interpretations for one and the same cluster. In the latter case, the observer has finally to weigh these interpretations based on neuroscientific arguments. We have performed both types of analysis here and found that the results are quite comparable. Intersubject variability has to be considered both in functional imaging of the cortex and in anatomical mapping. However, intersubject variability does not only represent a "problem" or "noise" influencing the data, but also contains important information about individual differences which can be quantified. This is a major advantage of probabilistic cytoarchitectonic maps.

Probabilistic maps are available in the format of the standard reference brain of the ECHBD (Roland and Zilles, 1994, 1996). They have also been transferred to the spatially normalized, T_1-weighted MR single-subject brain of the MNI (Evans et al., 1993; Collins et al., 1994; Holmes et al., 1998). These maps can be obtained via http://www.bic.mni.mcgill.ca/cytoarchitectonics// and http://www.fz-juelich.de/portal/oea_ime.

Acknowledgments

K.A. is supported by the Deutsche Forschungsgemeinschaft (Schn 362/13-1). J.M.G. and J.C.M. are supported by the Medical Research Council. G.R.F. and K.Z. are supported by the Deutsche Forschungsgemeinschaft (DFG-KFO 112). This Human Brain Project/Neuroinformatics research was funded jointly by the Human Brain Project Grant to the International Consortium for Brain Mapping (ICBM, P20-MHDA52176), funded by the National Institute of Mental Health, the National Institute of Neurological Disorders and Stroke, the National Institute of Drug Abuse, and the National Cancer Institute. We wish to thank Oliver Zafiris for technical support.

References

Aboitiz, F., Garcia, G.L., 1997. The evolutionary origin of language areas in the human brain. A neuroanatomical perspective. Brain Res. Rev. 25, 381–396.

Albert, M.L., Goodglass, H., Helm, N.A., Rubens, A.B., Alexander, M.P., 1981. Clinical Aspects of Dysphasia. Springer Verlag, Wien.

Amunts, K., Schleicher, A., Bürgel, U., Mohlberg, H., Uylings, H.B.M., Zilles, K., 1999. Broca's region revisited: cytoarchitecture and intersubject variability. J. Comp. Neurol. 412, 319–341.

Amunts, K., Schleicher, A., Zilles, K., 2002. Architectonic mapping of human cerebral cortex. In: Schüz, A., Miller, R. (Eds.), Cortical Areas: Unity and Diversity. Taylor and Francis, London, pp. 29–52.

Audenaert, K., Brans, B., Van Laere, K., Lahorte, P., Van Heeringen, K., 2000. Verbal fluency as a prefrontal activation probe: a validation study using ^{99m}Tc-ECD brain SPET. European Journal of Nuclear Medicine, vol. 27, pp. 1800–1808.

Baldo, J.V., Shimanura, A.P., 1998. Letter and category fluency in patients with frontal lobe lesions. Neuropsychology 12, 259–267.

Barbier, E.L., Marrett, S., Danek, A., Vortmeyer, A., van Gelderen, P., Duyn, J., Bandettini, P., Grafman, J., Koretsky, A.P., 2002. Imaging cortical anatomy by high-resolution MR at 3.0T: detection of the stripe of Gennary in visual area 17. Magn. Reson. Med. 48, 735–738.

Belin, P., Van Eeckhout, P., Zilbovicius, M., Remy, P., Francois, C., Guillaume, S., Chain, F., Rancurel, G., Samson, Y., 1996. Recovery from nonfluent aphasia after melodic intonation therapy: a PET study. Neurology 47, 1504–1511.

Ben-Shachar, M., Hendler, T., Kahn, I., Ben-Bashat, D., Grodzinsky, Y., 2003. The neural reality of syntactic transformation: evidence from fMRI. Psychol. Sci. 14, 433–440.

Binkofski, F., Amunts, K., Stephan, K.M., Posse, S., Schormann, T., Freund, H.-J., Zilles, K., Seitz, R.J., 2000. Broca's region subserves imagery of motion: a combined cytoarchitectonic and fMRI study. Hum. Brain Mapp. 11, 273–285.

Blank, S.C., Scott, S.K., Warburton, E.A., Wise, R.J.S., 2002. Speech production: Wernicke, Broca and beyond. Brain 125, 1829–1838.

Bookheimer, S.Y., 2002. Functional MRI of language: new approaches to understanding the cortical organization of semantic processing. Annu. Rev. Neurosci. 25, 151–188.

Bookheimer, S.Y., Zeffiro, T.A., Blaxton, T.A., Gaillard, P.W., Theodore, W.H., 2000. Activation of language cortex with automatic speech tasks. Neurology 55, 1151–1157.

Branche, C., Milner, B., Rasmussen, T., 1964. Intracarotid sodium amytal for the lateralization of cerebral speech dominance. J. Neurosurg. 21, 399–405.

Broca, M.P., 1861. Remarques sur le siége de la faculté du langage articulé, suivies d'une observation d'aphemie (Perte la parole). Bull. Mem. Soc. Anat. Paris 36, 330–357.

Brodmann, K., 1908. Beiträge zur histologischen Lokalisation der Großhirnrinde. VI: Die Cortexgliederung des Menschen. J. Psychol. Neurol. X, 231–246.

Brodmann, K., 1909. Vergleichende Lokalisationslehre der Großhirnrinde in ihren Prinzipien dargestellt auf Grund des Zellenbaues. Barth, JA, Leipzig.

Buckner, R.L., Raichle, M.E., Petersen, S.E., 1995. Dissociation of human prefrontal cortical areas across different speech production tasks and gender groups. J. Neurophysiol. 74, 2163–2173.

Caplan, D., Alpert, N., Waters, G., 1999. PET studies of syntactic processing with auditory sentence presentation. NeuroImage 9, 343–351.

Caplan, D., Alpert, N., Waters, G., Olivieri, A., 2000. Activation of Broca's area by syntactic processing under conditions of concurrent articulation. Hum. Brain Mapp. 9, 65–71.

Caramazza, A., 2000. Aspects of lexical access: evidence from aphasia. In: Grodzinsky, Y., Shapiro, L.P., Swinney, D. (Eds.), Language and the Brain. Academic Press, San Diego, CA, pp. 204–228.

Castaigne, P., 1979. Photographies et tomodensitométrie des deux cerveaux sur lesquels Broca fonda sa conception anatomoclinique de l' "aphémie". Bull. Acad. Natl. Med. 163, 663–667.

Clahsen, H., Featherstone, S., 1999. Antecedent priming at trace positions: evidence from German scrambling. J. Psychol. Res. 28, 415–437.

Collins, D.L., Neelin, P., Peters, T.M., Evans, A.C., 1994. Automatic 3-D intersubject registration of MR volumetric data in standardized Talairach space. J. Comput. Assist. Tomogr. 18, 192–205.

Crivello, F., Amunts, K., Tzourio-Mazoyer, N., Schormann, T., Roland, P.E., Zilles, K., Mazoyer, B., 2002. Functional segregation of Broca's region based on quantitative probabilistic cytoarchitectonic mapping of Brodmann's areas 44 and 45. NeuroImage 16, 128.

Curtis, V.A., Dixon, T.A., Morris, R.G., Bullmore, E.T., Brammer, M.J., Williams, S.C., Sharma, T., Murray, R.M., McGuire, P.K., 2001. Differential frontal activation in schizophrenia and bipolar illness during verbal fluency. J. Affect. Disord. 66, 111–121.

Dapretto, M., Bookheimer, S.Y., 1999. Form and content: dissociating syntax and semantics in sentence comprehension. Neuron 24, 427–432.

Demonet, J.F., Fiez, J.A., Paulesu, E., Petersen, S.E., Zatorre, R.J., 1996. PET studies on phonological processing: a critical reply to Poeppel. Brain Lang. 55, 352–379.

Desmond, J.E., Sum, J.M., Wagner, A.D., Demb, J.B., Shear, P.K., Glover, G.H., Gabrieli, J.D.E., Morrell, M.J., 1995. Functional MRI measurement of language lateralization in Wada-tested patients. Brain 118, 1411–1419.

Duvernoy, H., 1991. The Human Brain. Surface, Three-Dimensional Sectional Anatomy and MRI. Springer, Wien.

Embick, D., Marantz, A., Miyashita, Y., O'Neil, W.O., Sakai, K.L., 2000. A syntactic specialization for Broca's area. Proc. Natl. Acad. Sci. 97, 6150–6154.

Evans, A.C., Collins, D.L., Mills, S.R., Brown, E.D., Kelly, R.L., Peters, T.M., 1993. 3-D statistical neuroanatomical models from 305 MRI volumes. Nuclear Science Symposium and Medical Imaging Conference, 1993. 1993 IEEE Conference Record, San Francisco, CA, pp. 1813–1817.

Fatterpekar, G.M., Naidich, T.P., Delamn, B.N., Aguinaldo, J.G., Gultekin, S.H., Sherwood, C.C., Hof, P.R., Drayer, B.P., Fayad, Z.A., 2002. Cytoarchitecture of the human cerebral cortex: MR microscopy of excised specimens at 9.4 Tesla. Am. J. Neuroradiol. 23, 1313–1321.

Featherstone, S., Gross, M., Munte, T., Clahsen, H., 2000. Brain potentials in the processing of complex sentences: an ERP study of control and raising constructions. J. Psycholinguist. Res. 29, 141–154.

Fiez, J.A., 1997. Phonology, semantics, and the role of the left inferior prefrontal cortex. Hum. Brain Mapp. 5, 79–83.

Fletcher, P.C., Henson, R.N., 2001. Frontal lobes and human memory. Brain 124, 849–881.

Friederici, A.D., Mecklinger, A., 1995. Syntactic parsing as revealed by brain response. J. Psycholinguist. Res. 25, 157–176.

Friederici, A.D., Ruschemeyer, S.A., Hahne, A., Fiebach, C.J., 2003. The role of left inferior frontal and superior temporal cortex in sentence comprehension: localizing syntactic and semantic processes. Cereb. Cortex 13, 170–177.

Friston, K.J., Ashburner, J., Frith, C.D., Poline, J.-B., Heather, J.D., Frackowiak, R.S.J., 1995a. Spatial registration and normalization images. Hum. Brain Mapp. 3, 165–189.

Friston, K.J., Holmes, A.P., Worsley, K.J., Poline, J.-B., Frith, C.D., Frackowiak, R.S.J., 1995b. Statistical parametric maps in functional imaging: a general linear approach. Hum. Brain Mapp. 2, 189–210.

Frith, C.D., Friston, K.J., Liddle, P.F., Frackowiak, R.S.J., 1991a. A PET study of word finding. Neuropsychologia 29, 1148.

Frith, C.D., Friston, K.J., Liddle, P.F., Frackowiak, R.S.J., 1991b. Willed action and the prefrontal cortex in man: a study with PET. Proc. R. Soc. Lond. 244, 241–246.

Gabrieli, J.D.E., Poldrack, R.A., Desmond, J.E., 1998. The role of left prefrontal cortex in language and memory. Proc. Natl. Acad. Sci. 95, 906–913.

Goldman-Rakic, P.S., 1987. Circuitry of primate prefrontal cortex and regulation of behavior by representational memory. In: Mountcastle, V., Plum, F., Geige, S.V. (Eds.), Handbook of Physiology, Sect. 1, vol. 5. American Physiological Society, Bethesda, MD, pp. 373–417.

Goodglass, H., Fodor, I.G., Schulhoff, C., 1967. Prosodic factors in grammar—Evidence from aphasia. J. Speech Hear. 10, 5–20.

Groß, J., Ioannides, A.A., Dammers, J., Maeß, B., Friederici, A.D., Müller-Gärtner, H.-W., 1998. Magnetic field tomography analysis of continuous speech. Brain Topogr. 10, 273–281.

Gurd, J.M., Ward, C.D., 1989. Retrieval from semantic and letter-initial categories in patients with Parkinson's disease. Neuropsychologia 27, 743–746.

Gurd, J.M., Amunts, K., Weiss, P.H., Zafiris, O., Zilles, K., Marshall, J.C., Fink, G.R., 2002. Posterior parietal cortex is implicated in continuous switching between verbal fluency tasks: an fMRI study with clinical implications. Brain 125, 1024–1038.

Henn, S., Schormann, T., Engler, K., Zilles, K., Witsch, K., 1997. Elastische Anpassung in der digitalen Bildverarbeitung auf mehreren Auflösungsstufen mit Hilfe von Mehrgitterverfahren. In: Paulus, E., Wahl, F.M. (Eds.), Mustererkennung 1997. Springer, Informatik Aktuell, pp. 392–399.

Hinke, R.M., Hu, X., Stillman, A.E., Kim, S.G., Merkle, H., Salmi, R., Ugurbil, K., 1993. Functional magnetic resonance imaging of Broca's area during internal speech. NeuroReport 4, 675–678.

Holmes, C.J., Hoge, R., Collins, L., Woods, R., Toga, A.W., Evans, A.C., 1998. Enhancement of MR images using registration for signal averaging. J. Comput. Assist. Tomogr. 22, 324–333.

Horwitz, B., Amunts, K., Bhattacharyya, R., Patkin, D., Jeffries, J., Zilles, K., Braun, A.R., 2003. Activation of Broca's area during the production of spoken and signed language: a combined cytoarchitectonic mapping and PET analysis. Neuropsychologia 41, 1868–1876.

Indefrey, P., Brown, C.M., Hellwig, F., Amunts, K., Herzog, H., Seitz, R.J., Hagoort, P., 2001. A neural correlate of syntactic encoding during speech production. Proc. Natl. Acad. Sci. 98, 5933–5936.

Jahanshahi, M., Dirnberger, G., Fuller, R., Frith, C.D., 2000. The role of dorsolateral prefrontal cortex in random number generation: a study with positron emission tomography. NeuroImage 12, 713–725.

Janowsky, J., Shimanura, A.P., Kritchevsky, M., Squire, L.R., 1989. Cognitive impairment following frontal lobe damage and its relevance to human amnesia. Behav. Neurosci. 103, 548–560.

Keller, T., Carpenter, P.A., Just, M.A., 2001. The neural bases of sentence comprehension: a fMRI examination of syntactic and lexical processing. Cereb. Cortex 11, 223–237.

Knösche, T.R., Maeß, B., Friederici, A.D., 2000. Processing of syntactic information monitored by brain surface current density mapping based on MEG. Brain Topogr. 12, 75–87.

Koski, L., Wohlschlager, A., Bekkering, H., Woods, R.P., Dubeau, M.C., Mazziotta, J.C., Iacoboni, M., 2002. Modulation of motor and premotor activity during imitation of target-directed actions. Cereb. Cortex 12, 847–855.

Lezak, M., 1995. Neuropsychological Assessment. Oxford Univ. Press, Oxford.

Manjali, Z.M., Marshall, J.C., Stephan, K.E., Gurd, J.M., Zilles, K., Fink, G.R., 2003. In search of the hidden: an fMRI study with implications for the study of patients with autism and with acquired brain injury. NeuroImage 19, 674–683.

Mecklinger, A., Schriefer, H., Steinhauer, K., Friederici, A.D., 1995. Processing relative clauses varying on syntactic and semantic decisions: an analysis with event-related potentials. Mem. Cogn. 23, 477–494.

Merker, B., 1983. Silver staining of cell bodies by means of physical development. J. Neurosci. 9, 235–241.

Mohlberg, H., Weiss, P.H., Fink, G.R., Zilles, K., Amunts, K., 2002. Integration of a new non-linear elastic warping method and SPM99: verbal fluency and cytoarchitecture. NeuroImage 16, 492.

Mohlberg, H., Lerch, J., Amunts, K., Evans, A.C., Zilles, K., 2003. Probabilistic cytoarchitectonic maps transformed into MNI space. Presented at the 9th International Conference on Functional Mapping of the Human Brain, June 19–22 2003, New York. Available on CD ROM in NeuroImage, 19(2).

Mummery, C.J., Patterson, K., Hodges, J., Price, C.J., 1998. Organization of the semantic system-divisible by what? J. Cogn. Neurosci. 10, 766–777.

Ono, M., Kubik, S., Abernathey, C.D., 1990. Atlas of the Cerebral Sulci. Thieme, Stuttgart.

Owen, A.M., Downess, J.J., Sahakian, B.J., Polkey, C.E., Robbins, T.W., 1990. Planning and spatial memory following frontal lobe lesions in man. Neuropsychologia 28, 1021–1034.

Paulesu, E., Frith, C.D., Frackowiak, R.S.J., 1993. The neural correlates of the verbal component of working memory. Nature 362, 342–345.

Paus, T., Petrides, M., Evans, A.C., Meyer, E., 1993. Role of the human anterior cingulate cortex in the control of occulomotor, manual, and speech responses: a positron emission tomography study. J. Neurophysiol. 70, 453–469.

Poldrack, R.A., Wagner, A.D., Prull, M.W., Desmond, J.E., Glover, G.H. Gabrieli, J.D.E., 1999. Functional specialization for semantic and phonological processing in the left inferior prefrontal cortex. NeuroImage 10, 15–35.

Price, C.J., 1998. The functional anatomy of word comprehension and production. Trends Cogn. Sci. 2, 281–288.

Price, C.J., 2000. The anatomy of language: contributions from functional neuroimaging. J. Anat. 197, 335–359.

Rajkowska, G., Goldman-Rakic, P.S., 1995. Cytoarchitectonic definition of prefrontal areas in the normal human cortex: II. Variability in locations of areas 9 and 46 and relationship to the Talairach coordinate system. Cereb. Cortex 5, 323–337.

Ravnkilde, B., Videbech, P., Rosenberg, R., Gjedde, A., Gada, A., 2002. Putative tests of frontal lobe function: a PET-study of brain activation during Stroop's test and verbal fluency. J. Clin. Exp. Neuropsychol. 24, 534–547.

Roland, P.E., Zilles, K., 1994. Brain atlases—A new research tool. Trends Neurosci. 17, 458–467.

Roland, P.E., Zilles, K., 1996. The developing European computerized human brain database for all imaging modalities. NeuroImage 4, S39–S47.

Roland, P.E., Zilles, K., 1998. Structural divisions and functional fields in the human cerebral cortex. Brain Res. Rev. 26, 87–105.

Schleicher, A., Zilles, K., 1990. A quantitative approach to cytoarchitectonics: analysis of structural inhomogeneities in nervous tissue using an image analyser. J. Microsc. 157, 367–381.

Schleicher, A., Amunts, K., Geyer, S., Morosan, P., Zilles, K., 1999. Observer-independent method for microstructural parcellation of cerebral cortex: a quantitative approach to cytoarchitectonics. NeuroImage 9, 165–177.

Schlosser, R., Hunsche, S., Gawehn, J., Grunert, P., Vucurevic, G., Gesierich, T., Kaufmann, B., Rossbach, W., Stoeter, P., 2002. Characterization of BOLD-fMRI signal during a verbal fluency paradigm in patients with intracerebral tumors affecting the frontal lobe. Magn. Reson. Imaging 20, 7–16.

Schormann, T., Zilles, K., 1998. Three-dimensional linear and nonlinear transformations: an integration of light microscopical and MRI data. Hum. Brain Mapp. 6, 339–347.

Schormann, T., Dabringhaus, A., Zilles, K., 1995. Statistics of deformations in histology and improved alignment with MRI. IEEE Trans. Med. Imag. 14, 25–35.

Signoret, J.-L., Castaigne, P., Lhermitte, F., Abelanet, R., Lavorel, P., 1984. Rediscovery of Leborgne's brain: anatomical description with CT scan. Brain Lang. 22, 303–319.

Smith, C.D., Anderson, A.H., Kryscio, R.J., Schmitt, F.A., Kindy, M.S., Bloncer, L.X., Avison, M.J., 2002. Women at risk for AD show increased parietal activation during a fluency task. Neurology 58, 1197–1202.

Spence, S.A., Liddle, P.F., Stefan, M.D., Hellewell, J.S.E., Sharma, T., Friston, K.J., Hirsch, S.R., Frith, C.D., Murray, R.M., Deakin, J.F.W., Grasby, P.M., 2000. Functional anatomy of verbal fluency in people with schizophrenia and those at genetic risk. Focal dysfunction and distributed disconnectivity reappraised. Br. J. Psychiatry 176, 60.

Stephan, K.E., Marshall, J.C., Friston, K.J., Rowe, J.B., Ritzl, A., Zilles, K., Fink, G.R., 2003. Lateralized cognitive processes and lateralized task control in the human brain. Science 301, 384–386.

Talairach, J., Tournoux, P., 1988. Coplanar Stereotaxic Atlas of the Human Brain. Thieme, Stuttgart.

Thompson-Schill, S.L., D'Esposito, M., Aguirre, G.K., Farah, M.J., 1997. Role of left inferior prefrontal cortex in retrieval of semantic knowledge: a reevaluation. Proc. Natl. Acad. Sci. 94, 14792–14797.

Tomaiuolo, F., MacDonald, B., Caramanos, Z., Posner, G., Chiavaras, M., Evans, A.C., Petrides, M., 1999. Morphology, morphometry and probability mapping of the pars opercularis of the inferior frontal gyrus: an in vivo MRI analysis. Eur. J. Neurosci. 11, 3033–3046.

Uylings, H.B.M., Malofeeva, L.I., Bogolepova, I.N., Amunts, K., Zilles, K., 1999. Broca's language area from a neuroanatomical and developmental perspective. In: Hagoort, P., Brown, C. (Eds.), Neurocognition of Language Processing. Oxford Univ. Press, Oxford, pp. 319–336.

Vandenberghe, R., Price, C., Wise, R., Josephs, O., Frackowiak, R.S.J., 1996. Functional anatomy of a common semantic system for words and pictures. Nature 383, 254–256.

Walters, N., Egan, G.F., Kean, M., Jenkinson, M., Kril, J.J., Watson, J.D.G., 2003. In vivo identification of human cortical areas using high resolution MRI: an approach to structure-function correlation. Proc. Natl. Acad. Sci. 100, 2981–2986.

Wildgruber, D., Ackermann, H., Klose, U., Kardatzki, B., Grodd, W., 1996. Functional lateralization of speech production at primary motor cortex: a fMRI study. NeuroReport 7, 2791–2795.

Worsley, K.J., Marrett, S., Neelin, P., Vandal, A.C., Friston, K.J., Evans, A.C., 1996. A unified statistical approach for determining significant signals in images of cerebral activation. Hum. Brain Mapp. 4, 73.

Wree, A., Schleicher, A., Zilles, K., 1982. Estimation of volume fractions in nervous tissue with an image analyzer. J. Neurosci. Methods 6, 29–43.

Zatorre, R.J., Meyer, E., Gjedde, A., Evans, A.C., 1996. PET studies of phonetic processing of speech: review, replication, and reanalysis. Cereb. Cortex 6, 21–30.

Zilles, K., Palomero-Gallagher, N., Grefkes, C., Scheperjans, F., Boy, C., Amunts, K., Schleicher, A., 2002a. Architectonics of the human cerebral cortex and transmitter receptor fingerprints: reconciling functional neuroanatomy and neurochemistry. Eur. Neuropsychopharmacol. 12, 587–599.

Zilles, K., Schleicher, A., Palomero-Gallagher, N., Amunts, K., 2002b. Quantitative analysis of cyto- and receptor architecture of the human brain. In: Mazziotta, J.C., Toga, A. (Eds.), Brain Mapping: The Methods. Elsevier, USA, pp. 573–602.

Zurif, E., 2000. Brain regions of relevance to syntactic processing. In: Gleitman, L., Liberman, M. (Eds.), An Invitation to Cognition Science. MIT Press, Cambridge, MA, pp. 381–397.